JOURNAL OF GEOPHYSICAL RESEARCH, VOL. 97, NO. D16, PAGES 18,185–18,193, NOVEMBER 20, 1992

Annual Cycles of Tropospheric Water Vapor

DIAN J. GAFFEN

Air Resources Laboratory, National Oceanic and Atmospheric Administration, Silver Spring, Maryland, and Department of Meteorology, University of Maryland, College Park

ALAN ROBOCK

Department of Meteorology, University of Maryland, College Park

WILLIAM P. ELLIOTT

Air Resources Laboratory, National Oceanic and Atmospheric Administration, Silver Spring, Maryland

To understand better the annual cycles of atmospheric humidity, radiosonde data were used to create climatologies of temperature, dew point, relative humidity, and precipitable water in the lower troposphere for 56 locations around the world for the period 1973–1990. On the basis of the annual ranges of relative humidity at the surface and at the 850, 700, and 500 mbar levels and the ratio of the annual maximum to minimum surface to 500-mbar precipitable water, we have defined five humidity regimes: (1) middle- and high-latitude continental, (2) middle- and high-latitude oceanic, (3) mid-latitude monsoon, (4) tropical oceanic, and (5) tropical monsoon. For each regime we describe the annual cycles of temperature and humidity variables and discuss phase relationships among them. Relative humidity ranges are small in the first two regimes, where precipitable water and temperature vary in phase. Relative humidity ranges in the other three regimes are moderate to large, and in the tropics the annual march of horizontal moisture advection and vertical convection, not temperature, controls seasonal humidity variations. These results suggest that the assumption of constant relative humidity made in some climate models is not always justified and that precipitable water is not a strong function of temperature in the tropics.

INTRODUCTION

As a foundation for understanding long-term change in water vapor and related processes, the annual cycle of humidity must be understood. Investigations of the water vapor–greenhouse effect feedback [e.g., *Rind et al.*, 1991; *Raval and Ramanathan*, 1989] used seasonal and geographic variations as surrogates for long-term change. These studies employed satellite water vapor and radiation data, respectively, and the shortness of the satellite record did not allow testing the assumption that seasonal and spatial changes reveal patterns of long-term change.

Surprisingly, there are few studies in the literature of the observed annual cycle of humidity above the surface. A few early investigators [*Reitan* 1960*a*, *b*; *Bannon and Steele*, 1960; *Tuller*, 1968] used radiosonde observations to characterize seasonal variations in precipitable water (PW) but did not consider other measures of water vapor or their vertical profiles. Later work showed seasonal variations in specific humidity [*Rasmusson*, 1972; *Peixoto et al.*, 1981; *Peixoto and Oort*, 1983; *Oort*, 1983] but was based on radiosonde data that were (1) taken before 1973, which are known to be of poor quality relative to more modern measurements, (2) gridded or zonally averaged, which is likely to mask local variability in humidity, or (3) compiled into monthly means, which cannot be used to derive supplemental humidity variables without introducing bias [*Elliott and Gaffen*, 1991].

Using microwave observations from the Nimbus 7 satellite, *Prabhakara et al.* [1985] presented seasonal maps of PW over the open oceans for 1979–1981 and confirmed the general global patterns deduced from radiosonde-based studies but with much more detail in the tropics and southern oceans. Later studies by *Liu* [1986] and *Liu and Niiler* [1990] have focused on variations of surface relative humidity and PW at oceanic sites with an eye toward improved parameterization of ocean-atmosphere fluxes using remotely sensed PW. Recently, the seasonal cycles of clear sky upper tropospheric relative humidity have been determined from measurements in the thermal infrared by Meteosat [*van de Berg et al.*, 1991] and by the Stratospheric Aerosol and Gas Experiment (SAGE II) [e.g., *Chiou et al.*, 1992]. Because these satellite observations are possible in clear skies only, the annual cycle may not be fully resolved in regions with a distinct cloudy season.

While earlier studies have focused on particular aspects of tropospheric humidity, none has explicitly explored the annual cycle of both relative and specific humidity at a representative sample of stations globally. Using radiosonde data, we examine the local annual cycles of the major humidity variables, which leads us to the identification of five distinct water vapor regimes. Then seasonal variations in relative humidity are explained and interpreted in greater detail.

DATA AND METHOD

Daily radiosonde reports, provided by National Climatic Data Center (tape deck 6103), from January 1973 through December 1990, formed the basic data set. The 56 stations selected (Figure 1 and Table 1) are a subset of the 63-station

Paper number 92JD01999.
0148-0227/92/92JD-01999$05.00

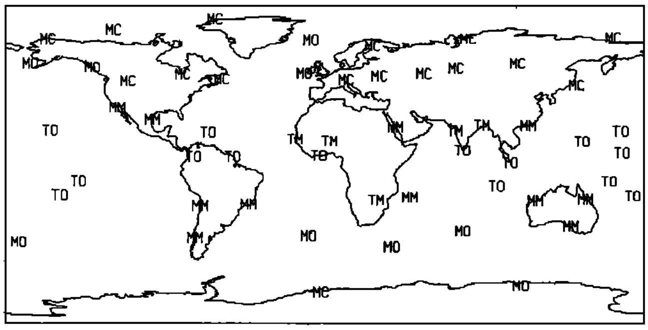

Fig. 1. Map of the humidity regimes of each radiosonde station studied. The regimes are middle- and high-latitude continental (MC), middle- and high-latitude oceanic (MO), mid-latitude monsoon (MM), tropical oceanic (TO), and tropical monsoon (TM).

network described and used by *Angell and Korshover* [1983] for analysis of tropospheric and stratospheric temperature. However, *Elliott et al.* [1991] identified some problems with the original 63-station set for the analysis of humidity data. Thirty-nine of the 56 stations used here have very few missing data, at least for one observation time per day. The other 17 were included to give reasonable global representation of climatic zones, even though they could not be used for the full 18 years.

The radiosonde report includes temperature (T) and dew point depression at all levels, geopotential height of mandatory levels, and surface pressure and pressure of other significant levels. These were converted to dew point (T_d) and relative humidity (RH) at each level and precipitable water (PW) in the surface to 850 mbar ($PW_{s\text{-}8}$) and surface to 500-mbar ($PW_{s\text{-}5}$) layers. Precipitable water is a measure of column water vapor content and is the integral between two pressure levels (p_1 and p_2) of specific humidity (q):

$$PW = -\frac{1}{g}\int_{p_1}^{p_2} q\,dp \tag{1}$$

where g is the gravitational acceleration. Because of the known poor performance of radiosonde hygristors in cold, dry environments, and because almost all of the water vapor in the atmosphere is in the lower troposphere, no data above 500 mbar were used. Details on data quality control are given by *Gaffen* [1992].

For each station, observation time (0000 and 1200 UT), and variable, monthly means were calculated from the daily data. To characterize the mean annual cycles, the 18 years of monthly means were averaged to obtain long-term monthly means.

To measure the amplitude of the annual cycles, the ranges of monthly mean RH were computed as the difference between the maximum and minimum long-term monthly mean values. A PW ratio was defined as the ratio of the maximum to minimum long-term monthly mean $PW_{s\text{-}5}$. In addition, the surface temperature (T_s) range and mean annual T_s and $PW_{s\text{-}5}$ were computed. To analyze phase relationships among variables, the months in which annual minima and maxima occurred were recorded. Two variables were considered to be in phase when the maximum and minimum of one occurred within one month of the maximum and minimum of the other.

HUMIDITY REGIMES

Examining the data for the individual stations revealed five natural categories into which the stations could be classified, on the basis of the annual RH ranges at the various levels, the PW ratio, and the phase relationships between PW and other variables. Because the stations in

TABLE 1. Radiosonde Station Names, World Meteorological Organization Identification Numbers, Locations, and Elevations (m)

Identification	Name	Latitude	Longitude	Elevation
01001	Jan Mayen	70.9	−8.7	9
02836	Sodankla	67.3	26.7	178
03953	Valentia	51.9	−10.3	14
10868	Munich	48.2	11.7	484
20674	Dikson	73.5	80.2	20
21965	Chetyrekhstolbovy	70.7	162.3	6
28698	Omsk	54.9	73.2	91
30230	Kirensk	57.8	108.2	257
33345	Kiev	50.3	30.5	166
35121	Orenburg	51.8	55.2	109
40477	Jeddah	21.7	39.2	18
42809	Calcutta	22.5	88.3	5
43003	Bombay	19.2	72.8	11
43371	Trivandrum	8.5	77.0	64
45004	Hong Kong	22.3	114.2	62
47401	Wakkanai	45.3	141.7	3
48698	Singapore	1.4	104.0	3
61052	Niamey	13.5	2.2	233
61641	Dakar	14.7	−17.5	24
61996	New Amsterdam	−37.8	77.5	29
65578	Abidjan	5.3	−3.9	7
67083	Antananarivo	−18.8	47.5	1276
67964	Bulawayo	−20.2	28.7	1344
68906	Gough	−40.3	−9.8	54
68994	Marion	−46.8	37.8	22
70026	Barrow	71.3	−156.8	4
70308	St. Paul	57.2	−170.2	9
70398	Annette	55.0	−131.5	34
71072	Mould Bay	76.2	−119.3	12
71082	Alert	82.5	−62.3	63
71815	Stephenville	48.5	−58.5	26
71836	Moosonee	51.3	−80.7	10
72250	Brownsville	25.8	−97.5	6
72290	San Diego	32.7	−117.2	9
72775	Great Falls	47.5	−111.3	1115
78526	San Juan	18.5	−66.0	3
80222	Bogota	4.7	−74.2	2541
81405	Cayenne	4.8	−52.3	9
83746	Rio de Janeiro	−22.8	−43.2	5
85442	Antofagasta	−23.5	−70.5	137
85799	Puerto Montt	−41.5	−73.2	90
89001	S.A.N.A.E.	−70.3	−2.3	52
89611	Casey	−66.3	110.7	9
91217	Guam	13.5	144.8	111
91245	Wake	19.3	166.7	4
91285	Hilo	19.7	−155.0	10
91376	Majuro	7.0	171.3	3
91517	Honiara	−9.3	160.0	55
91680	Nandi	−17.7	177.5	18
91925	Atuona	−9.8	−139.0	52
91938	Tahiti	−17.5	−149.7	2
93986	Chatham	−43.9	−176.5	48
94294	Townsville	−19.3	146.8	5
94312	Port Hedland	−20.3	118.7	6
94672	Adelaide	−34.9	138.5	4
96996	Cocos	−12.2	96.8	3

Positive latitude and longitude are degrees north and east, respectively.

TABLE 2. Amplitudes and Phase Relationships of the Annual Cycles of Tropospheric Humidity for the Five Humidity Regimes

Humidity Regime	PW Ratio	RH Range*	Variables in Phase With PW
Middle- and high-latitude continental	3–9	small†	T and T_d at all levels
Middle- and high-latitude oceanic	1.5–3	small	T and T_d at all levels
Mid-latitude monsoon	1.3–3	moderate or large moderate in PBL†‡	T and T_d at all levels, midtropospheric RH
Tropical oceanic	1–1.6	moderate or large small in PBL‡	Midtropospheric RH and T_d
Tropical monsoon	2–3	large	Midtropospheric RH and T_d

PW ratio is the ratio of the maximum to minimum monthly mean values of surface to 500-mbar precipitable water. RH range is the difference between maximum and minimum monthly mean relative humidity, evaluated at the surface and at the 850, 700, and 500 mbar levels.

*The ranges are categorized as small, ≤15%; moderate, 15–30%; and large, 30–60%.

†Daytime surface relative humidity does not always follow these patterns and can exhibit a moderate annual range.

‡The surface and 850-mbar level represent the planetary boundary layer (PBL).

each regime tended to have geographic similarities, we named them accordingly.

Poleward of about 20° latitude, where the annual cycles of T and PW are in phase, most stations have small RH ranges. A subset of these with high PW ratios we designate the middle- and high-latitude continental regime. The subset with less annual variation of PW, found along windward coasts or on islands, is called the middle- and high-latitude oceanic regime. The third mid-latitude regime also shows modest annual changes in PW but sizable annual ranges of RH. These stations have a distinct rainy season and so were grouped as the mid-latitude monsoon regime.

Stations between 20°N and 20°S have distinct annual cycles in PW but not in T. The tropical oceanic regime is characterized by a small PW ratio and small RH ranges in the planetary boundary layer (PBL) but substantial variations in RH in the midtroposphere. (In this analysis, the surface and 850-mbar data are considered representative of the PBL, and the 700- and 500-mbar levels are considered the midtroposphere.) The tropical monsoon regime stations have larger PW ratios and a larger RH range throughout the lower troposphere. The stations are identified by their regimes in Figure 1, and the quantitative limits of the RH ranges and PW ratios are given in Table 2.

In the remainder of this section we describe additional features of these humidity regimes and show an example of each. Where available, we show nighttime data because in the middle- and high-latitude continental and mid-latitude monsoon regimes, daytime surface RH is often more variable than RH aloft or than surface RH at night. (The influence of the land surface as a source of moisture, and the possibility of evaporation being less than its potential value, probably accounts for this daytime variability in surface RH in these two regimes.) Therefore we relied more on nighttime than on daytime surface RH variability to determine a station's water vapor regime, although some stations, particularly in the tropics, have only daytime observations.

Middle- and High-Latitude Continental Humidity Regime

The middle- and high-latitude continental (MC) humidity regime is characterized by a pronounced annual cycle in PW and small variations in RH. Munich, Germany, is a good example of the MC regime (Figure 2). Both $PW_{s\text{-}8}$ and $PW_{s\text{-}5}$ reach a maximum in late summer, as do both T and T_d. At MC stations, summer $PW_{s\text{-}5}$ can be 3 to 10 times greater than winter $PW_{s\text{-}5}$, while boundary layer and midtropospheric RH ranges are generally less than 15%.

Although not used to classify stations, the annual mean and annual range of T_s and the annual mean $PW_{s\text{-}5}$ provide additional distinguishing characteristics of each regime. The MC sites exhibit large annual ranges in T_s, more than 20°C, and low annual mean T_s, less than 10°C. As one would expect, on the basis of the Clausius-Clapeyron relation, annual mean $PW_{s\text{-}5}$ is also low, 0.2 to 1.5 cm.

Middle- and High-Latitude Oceanic Humidity Regime

Qualitatively resembling the MC regime, the middle- and high-latitude oceanic (MO) regime shows the moderating and moistening influences of the ocean. Island and coastal stations poleward of 40° tend to show MO characteristics (Figure 1), and Valentia, Ireland, is a typical example (Figure 3). At MO sites, RH ranges are small, particularly above the PBL where they tend to be less than 10%. This, combined with small annual T_s ranges (less than 15°C), results in smaller $PW_{s\text{-}5}$ ratios (1.5 to 3) than at MC sites. As at MC sites, T, T_d, and PW are in phase, peaking in summer. Annual mean T_s is generally less than 15°C, and annual mean $PW_{s\text{-}5}$ is 0.5 to 2.0 cm. Jan Mayen Island, at 70.6°N, and Casey, Antarctica, at 66.2°S, are, respectively, the most northerly and southerly MO stations.

The smaller T_s range and PW ratio at MO stations compared with MC stations are consistent with the findings of *Reitan* [1960*a*, *b*], who noted that the PW ratio is a good indicator of continentality, commonly expressed as the annual range of temperature. *Peixoto et al.* [1981] also found seasonal changes in surface to 300-mbar PW more marked over land than over sea.

Mid-Latitude Monsoon Humidity Regime

The mid-latitude monsoon (MM) stations are coastal sites between about 20° and 40° latitude and show more annual variability in RH than either MC or MO stations. At Rio de Janeiro, Brazil, for example, surface RH is maximum in winter, but aloft RH is maximum in summer, in phase with T, T_d, and PW (Figure 4). This summertime maximum in midtropospheric humidity corresponds with a summertime maximum in precipitation [*Eischeid et al*, 1991]. The seasonal humidity variations at MM stations are related to

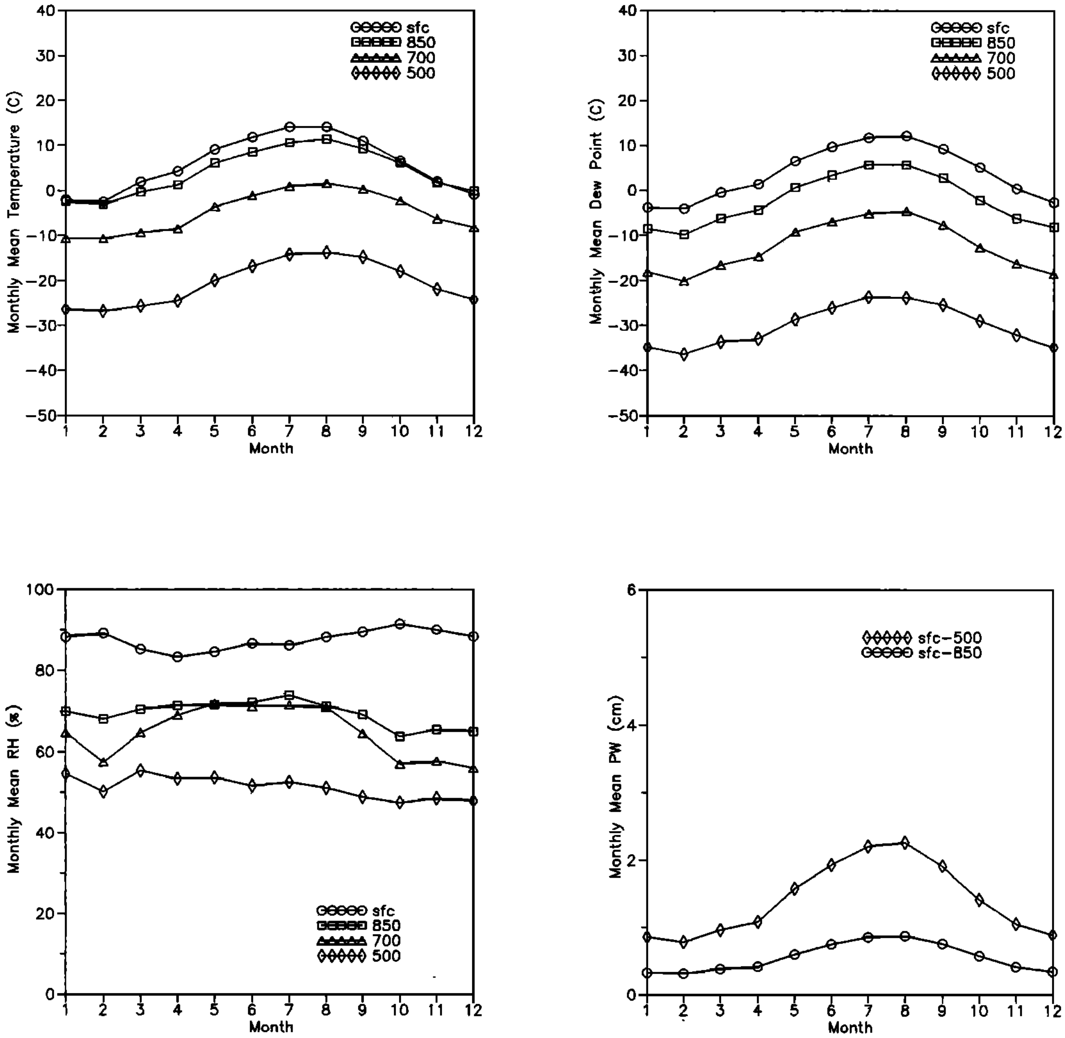

Fig. 2. The annual cycles of temperature, dew point, relative humidity (at the surface and at 850, 700, and 500 mbar), and precipitable water (in the layers surface to 850 mbar and surface to 500 mbar) at Munich, Germany, at 0000 UT. Data are long-term monthly means for the period 1973–1986. Munich is an example of the middle- and high-latitude continental humidity regime.

seasonal circulation and convection patterns, so the term "monsoon" is appropriate for the regime.

At MM stations, RH ranges can approach 50%, both in the PBL and the midtroposphere. Ratios of $PW_{s\text{-}5}$ are comparable to the MO stations, 1.3 to 3. At MM stations, annual mean $PW_{s\text{-}5}$ is between 1.4 and 4.0 cm, and annual mean T_s is typically greater than 15°C, with annual ranges of 5° to 13°C.

Tropical Oceanic Humidity Regime

In marked contrast to the MC, MO, and MM regimes, the tropical oceanic (TO) regime is characterized by a PBL with a relatively constant moisture content and a more variable midtroposphere. Wake Island is a typical TO station (Figure 5). Boundary layer T and T_d are in phase, with a slight maximum in the summer. They combine to give a uniformly moist PBL, as seen in the RH data, resulting in high PW in the surface to 850-mbar layer, greater than 2 cm. The annual range of T in the midtroposphere is negligible, but T_d varies by more than 10°C, leading to RH ranges of about 30%. The high midtropospheric RH in summer and fall is associated with the rainy season at Wake [*National Oceanic and Atmospheric Administration*, 1982]. As a result, most of the annual change in PW is above 850 mbar, and $PW_{s\text{-}5}$ is in phase with midtropospheric T_d and RH.

At TO stations the ratio of maximum to minimum $PW_{s\text{-}5}$ is less than 1.6, and monthly mean PBL RH is high, always above 60%, with a small annual range. Midtropospheric RH is lower than in the PBL (in fact, a monotonic decrease of RH with decreasing pressure is noted in most regimes), but it is more variable; the annual range can approach 50%. For TO stations, annual mean T_s is generally greater than 20°C, and annual range of T_s is less than 5°C, warm all year. Annual mean $PW_{s\text{-}5}$ at TO sites is high, 3 to 5 cm. All TO stations are within 20° of the equator and are either island or coastal sites (Figure 1).

The PW ratios we compute are comparable to what we infer from *Prabhakara et al.* [1985] and *Liu* [1986] for the tropical Pacific. Our results are also consistent with those of *Liu and Niiler* [1990], who found tropical oceanic surface RH to vary by less than 10% over the course of the year and to be generally between 70 and 80%. The RH variability

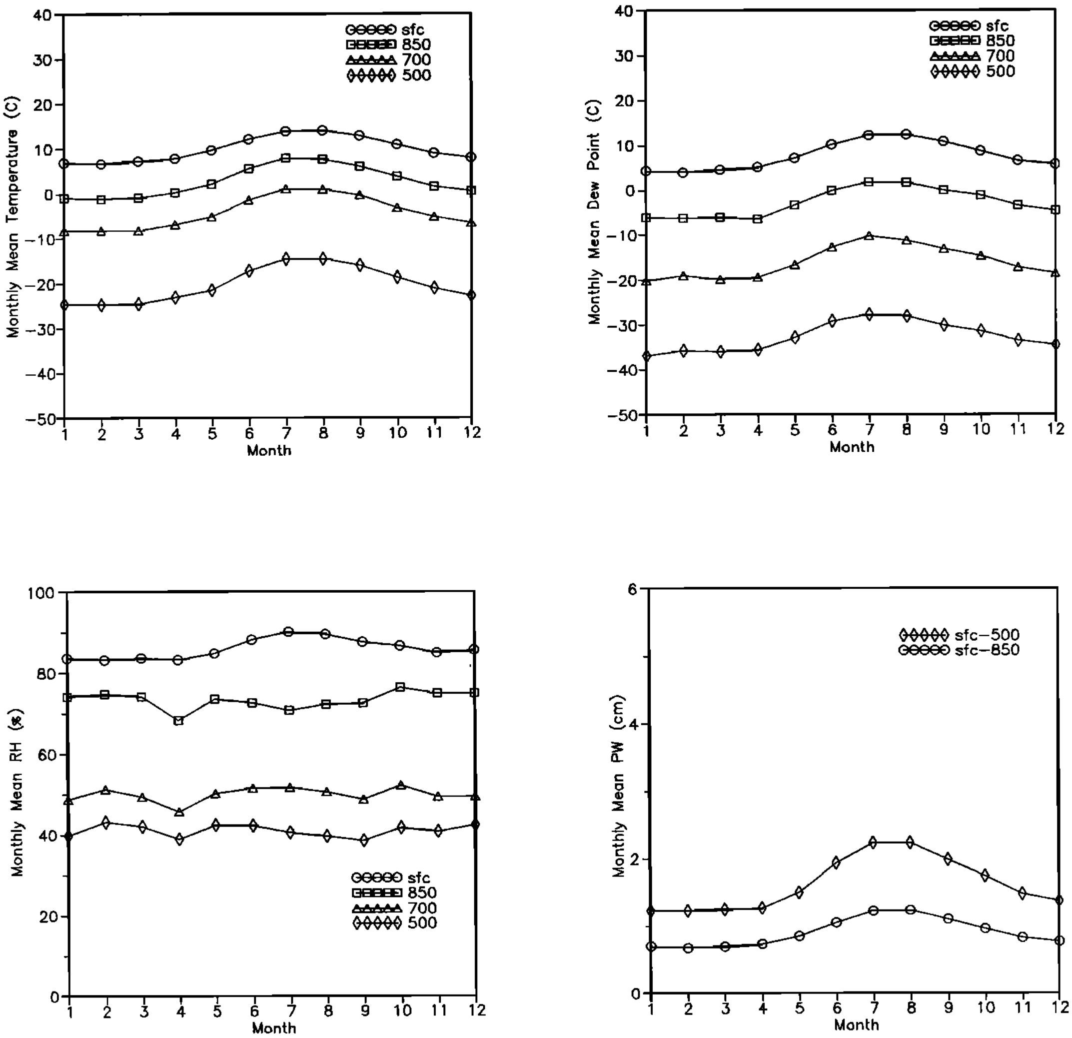

Fig. 3. Same as Figure 2 but for Valentia, Ireland. Data are long-term 0000 UT monthly means for the period 1973–1990. Valentia is an example of the middle- and high-latitude oceanic humidity regime.

above the PBL can be compared with the results of *Rasmusson* [1972], who noted that zonally averaged RH showed maximum January to July changes, in excess of 20%, in the subtropical midtroposphere. Our RH range is larger probably because we are not taking a zonal mean. The large-scale cause of these seasonal changes is probably seasonal changes in convective activity and precipitation associated with the north-south movement of the intertropical convergence zone, as suggested by *Prabhakara et al.* [1979].

Tropical Monsoon Humidity Regime

Much more seasonal variability is evident in tropical monsoon (TM) locations. There are two subtypes of the TM regime. The first is the humid coastal climate, for example Bombay, India, where the boundary layer remains humid all year but the midtroposphere has a distinct dry season. The second is an inland regime, as at Niamey, Niger (Figure 6), where the dry season is evident at all levels. In both subtypes, midtropospheric T shows little variation, but PBL T has a minimum in winter and a secondary summer minimum when T_d is maximum. The secondary minimum during the moist season is probably due to the surface cooling effects of cloud cover and precipitation. As in the MM and TO regimes, seasonal variations in convection and in moisture advection, related to large-scale atmospheric circulation patterns, control seasonal humidity variations at TM sites.

At TM stations, $PW_{s\text{-}5}$ ratios are between 2 and 3. In both the PBL and midtroposphere, RH ranges are large, generally greater than 30%. Annual mean $PW_{s\text{-}5}$ at these sites is 1.5 to 5 cm. Annual mean T_s is high, 15° to 30°C, with annual ranges between 4° and 12°C.

SEASONAL CHANGES IN RELATIVE HUMIDITY

The assumption that RH is approximately constant, both over the course of the year and over longer periods, is often made and formed the basis of the early modeling study of the effects of increasing atmospheric carbon dioxide by *Manabe and Wetherald* [1967]. They argued that holding RH constant in a radiative-convective climate model is more reasonable than holding absolute humidity constant, on the basis of observations of both humidity variables. They showed figures from *Telegadas and London* [1954] as evidence that relative humidity changes little over the course of the year.

Close examination of those figures, and of figures pre-

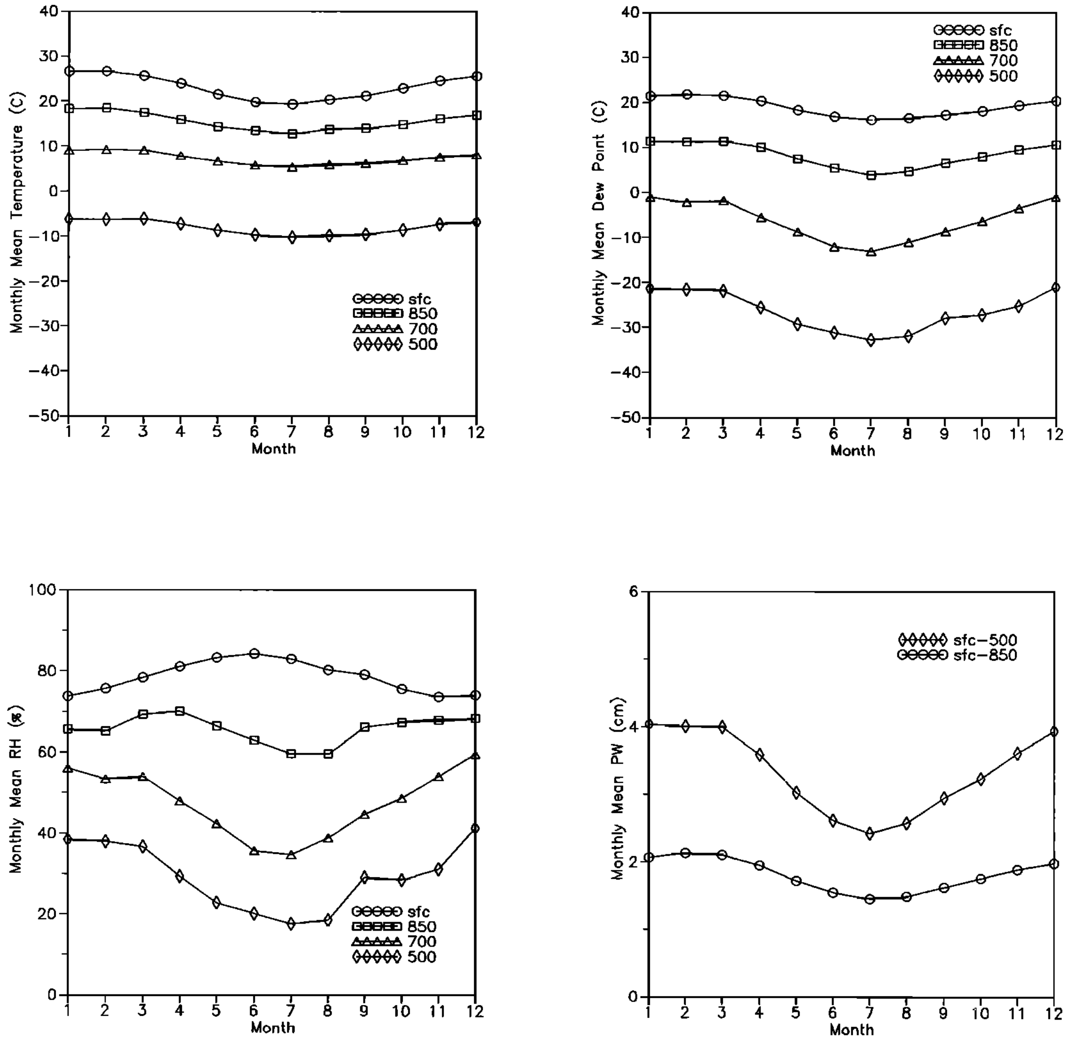

Fig. 4. Same as Figure 2 but for Rio de Janeiro, Brazil. Data are long-term 1200 UT monthly means for the period 1973–1990. Rio de Janeiro is an example of the mid-latitude monsoon humidity regime.

sented by *Rasmusson* [1972], *Rind et al.* [1991], and *Chiou et al.* [1992], reveals that summer to winter RH changes as large as 20% are typical in some regions of the troposphere for zonally averaged RH for seasons or representative months. Furthermore, from the above analysis of station data, it is clear that lower tropospheric RH can range over 50% locally over the course of a year. To understand better the nature of the annual cycle of RH, this section presents an expression for the time rate of change of RH and discusses it in terms of the water vapor regimes described above.

Relative humidity does not vary independently but is a result of the combined effects of T and T_d:

$$\mathrm{RH} = \frac{e_s(T_d)}{e_s(T)} \tag{2}$$

where e_s is the saturation vapor pressure. Using the Clausius-Clapeyron equation, we can express e_s as

$$e_s(T) = e_0 \exp\left[\frac{L}{R_v}\left(\frac{1}{T_0} - \frac{1}{T}\right)\right] \tag{3}$$

where L is the latent heat of vaporization, taken to be constant, R_v is the gas constant for water vapor, $e_0 = e_s(T_0)$, and $T_0 = 273$ K. The time rate of change of RH is then given by

$$\frac{\partial \mathrm{RH}}{\partial t} = \frac{L}{R_v}\,\mathrm{RH}\left[\frac{1}{T_d^2}\frac{\partial T_d}{\partial t} - \frac{1}{T^2}\frac{\partial T}{\partial t}\right] \tag{4}$$

Of course, here we are not considering the day-to-day variations in T, T_d, and RH; rather, we are taking monthly mean values of each variable as representative of the daily values and considering month-to-month changes in the means. To gain some insight into the processes that can lead to seasonal changes in RH, we consider the two cases of approximately constant and of seasonally varying RH.

Approximately Constant Relative Humidity

If

$$\frac{\partial \mathrm{RH}}{\partial t} \approx 0 \tag{5}$$

then

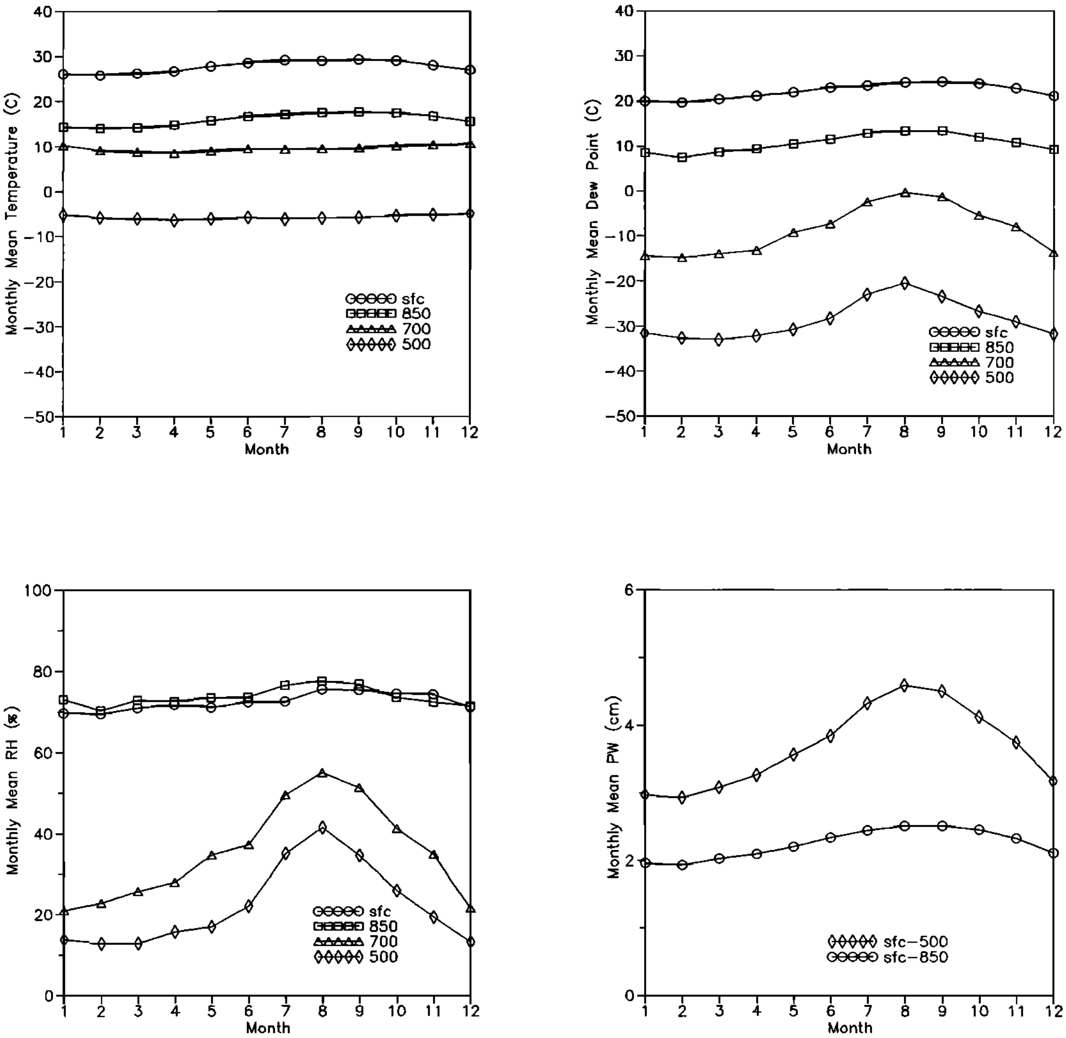

Fig. 5. Same as Figure 2 but for Wake Island. Data are long-term 0000 UT monthly means for the period 1973–1990. Wake Island is an example of the tropical oceanic humidity regime.

$$\frac{1}{T_d^2}\frac{\partial T_d}{\partial t} \approx \frac{1}{T^2}\frac{\partial T}{\partial t} \tag{6}$$

Since T_d can never exceed T, the time rate of change of T_d must be slightly less than that of T, and this discrepancy grows as RH decreases.

The water vapor regimes that exhibit minimal RH changes over the course of the year are the MC and MO regimes and the TO regime in the PBL. In the latter tropical case, PBL T and T_d are almost constant, so (6) is satisfied because both sides are approximately zero. In the MC and MO regimes, T and T_d vary in phase, therefore their time rates of change always have the same sign. At Valentia (Figure 3), seasonal changes in T and T_d are almost identical, but at Munich (Figure 2) the time rate of change of T exceeds that of T_d, as required by (6).

Relative Humidity Varies Seasonally

From (4) it follows that when RH increases with time,

$$\frac{1}{T_d^2}\frac{\partial T_d}{\partial t} > \frac{1}{T^2}\frac{\partial T}{\partial t} \tag{7}$$

and when RH decreases with time,

$$\frac{1}{T_d^2}\frac{\partial T_d}{\partial t} < \frac{1}{T^2}\frac{\partial T}{\partial t} \tag{8}$$

There are two possible scenarios.

Dew point variations greater than temperature variations. If T is approximately constant, as at TO stations above the PBL, then (4) requires that T_d and RH be in phase, as observed (e.g., at Wake Island, Figure 5). Even if T variations are not negligible, when T_d variations are much larger, RH cannot be constant. In the TM regime the midtroposphere experiences a period of increasing T_d and RH as the humid season approaches and a period of decreasing T_d and RH as the dry season approaches. At Niamey, for example (Figure 6), 700- and 500-mbar T changes are minimal compared with T_d changes. The changes are consistent with (7) and (8), with T_d increasing faster than T as the moist summer season approaches and decreasing faster than T as the dry season approaches.

Large temperature variations. If there is a pronounced seasonal cycle in T, as at MM stations, T and T_d vary in phase with RH, but the time rate of change of T_d is greater

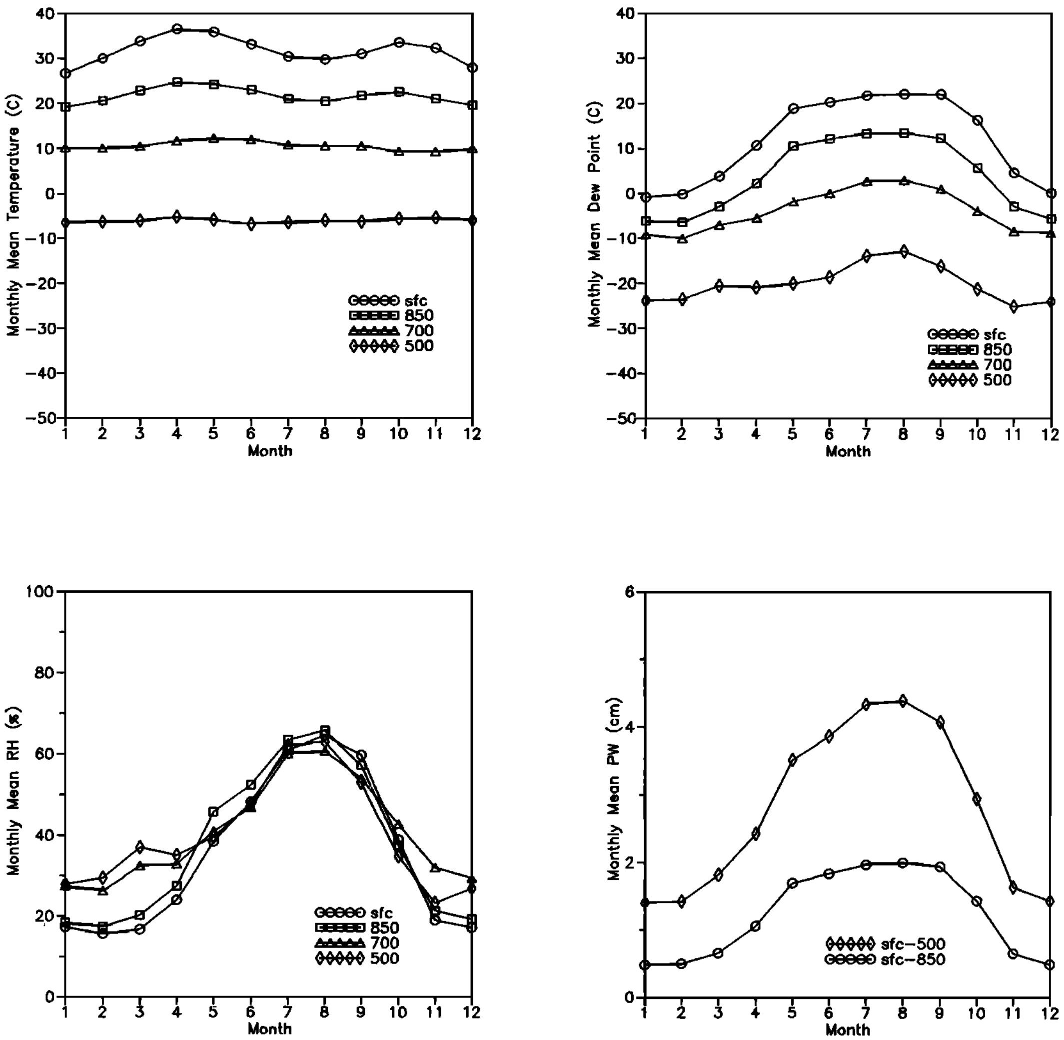

Fig. 6. Same as Figure 2 but for Niamey, Niger. Data are long-term 1200 UT monthly means for the period 1973–1990. Niamey is an example of the tropical monsoon humidity regime.

(in absolute magnitude) than that of T (e.g., at Rio de Janeiro, Figure 4). Thus the advection of moisture (as measured by T_d) by the monsoon circulation is more significant than thermal (T) advection for determining RH variations at both tropical and mid-latitude monsoon stations.

DISCUSSION

Examining the annual march of RH at stations around the globe reveals different patterns at different locations. In middle and high latitudes, RH is approximately constant throughout the year, except at locations influenced by monsoon circulations. But in low-latitude regions, horizontal and vertical moisture advection, combined with low-amplitude changes in T over the course of the year, allows for substantial seasonal variation in RH. This is especially true above the PBL, which highlights the need for analysis of humidity measurements above the surface.

The annual cycles of PW are consistent with the RH patterns. In middle and high latitudes, PW follows T. In the tropics, however, the annual cycle of PW is more closely related to midtropospheric RH variations than to T variations and reaches maximum values during the local rainy season when deep convection is strong. Our results for the troposphere below 500 mbar are qualitatively consistent with RH variations at higher levels measured by satellites [*van de Berg et al.*, 1991; *Chiou et al.*, 1992], that is, larger variations in the tropics than at mid-latitudes. While these five regimes are quite clearly delineated in our 56-station data set, future work will establish whether they are sufficient to characterize the annual cycles of tropospheric humidity globally.

The existence of distinct humidity regimes suggests that a single set of assumptions above the vertical structure of humidity, and its seasonal variations, should not be applied globally. One-dimensional climate models need to distinguish between tropical and mid-latitude and between continental and oceanic atmospheres not just in terms of temperature profiles but also in terms of humidity profiles. Our results can also help to evaluate three-dimensional climate model simulations of the global climatology of tropospheric water vapor.

If one wishes to draw analogies between long-term changes in climate and seasonal variations in the present climate, the assumption that PW will increase as T increases and RH remains constant might be valid at some middle- and high-latitude locations. However, it cannot be supported in tropical regions at least at individual stations.

REFERENCES

Angell, J. K., and J. Korshover, Global temperature variations in the troposphere and stratosphere, 1958–1982, *Mon. Weather Rev.*, *111*, 901–921, 1983.

Bannon, J. K., and L. P. Steele, Average water-vapour content of the air, *Geophys. Mem. 102*, U.K. Meteorol. Office, London, 1960.

Chiou, E. W., J. C. Larsen, M. P. McCormick, W. P. Chu, and D. Rind, Global distributions of upper tropospheric relative humidity derived from SAGE II observations, paper presented at 72nd American Meteorological Society, Annual Meeting, Am. Meteorol. Soc., Boston, Mass., Jan 5–10, 1992.

Eischeid, J. K., H. F. Diaz, R. S. Bradley, and P. D. Jones, A comprehensive precipitation data set for global land areas, *DOE/ER-69017T-H1*, 81 pp., U.S. Dep. of Energy, Washington, D. C., 1991.

Elliott, W. P., and D. J. Gaffen, On the utility of radiosonde humidity archives for climate studies, *Bull. Am. Meteorol. Soc.*, *72*, 1507–1520, 1991.

Elliott, W. P., M. E. Smith, and J. K. Angell, On monitoring tropospheric water vapor changes using radiosonde data, in *Greenhouse-Gas-Induced Climatic Change: A Critical Appraisal of Simulations and Observations*, edited by M. Schlesinger, pp. 311–328, Elsevier, New York, 1991.

Gaffen, D. J., Observed annual and interannual variations in tropospheric water vapor, Ph.D. dissertation, Univ. of Md., College Park, 1992.

Liu, W. T., Statistical relation between monthly mean precipitable water and surface-level humidity over global oceans, *Mon. Weather Rev.*, *114*, 1591–1602, 1986.

Liu, W. T., and P. P. Niiler, The sensitivity of latent heat flux to the air humidity approximations used in ocean circulation models, *J. Geophys. Res.*, *95*, 9745–9753, 1990.

Manabe, S., and R. T. Wetherald, Thermal equilibrium of the atmosphere with a given distribution of relative humidity, *J. Atmos. Sci.*, *24*, 241–259, 1967.

National Oceanic and Atmospheric Administration, *Local Climatological Data: Annual Summaries for 1982*, vol. 1 and 2, National Climatic Data Center, Asheville, N. C., 1982.

Oort, A. H., Global atmospheric circulation statistics, 1958–1973, *NOAA Prof. Pap. 14*, 180 pp., Natl. Oceanic and Atmos. Admin., U.S. Dep. of Commer., Washington, D. C., 1983.

Peixoto, J. P., and A. H. Oort, The atmospheric branch of the hydrological cycle and climate, in *Variations in the Global Water Budget*, edited by A. Street-Perrott, M. Beran, and R. Ratcliffe, pp. 5–65, D. Reidel, Hingham, Mass., 1983.

Peixoto, J. P., D. A. Salstein, and R. D. Rosen, Intraannual variation in large-scale moisture fields, *J. Geophys. Res.*, *86*, 1255–1264, 1981.

Prabhakara, C., G. Dalu, R. C. Lo, and N. R. Nath, Remote sensing of seasonal distribution of precipitable water vapor over the oceans and the interference of boundary-layer structure, *Mon. Weather Rev.*, *107*, 1388–1401, 1979.

Prabhakara, C., D. A. Short, and B. E. Volmer, El Niño and atmospheric water vapor: Observations from Nimbus 7 SMMR, *J. Clim. Appl. Meteorol.*, *24*, 1311–1324, 1985.

Rasmusson, E. M., Seasonal variation of tropical humidity parameters, in *The General Circulation of the Tropical Atmosphere*, vol. 1, edited by R. E. Newell et al., pp. 193–237, MIT Press, Cambridge, Mass., 1972.

Raval, A., and V. Ramanathan, Observational determination of the greenhouse effect, *Nature*, *342*, 758–761, 1989.

Reitan, C. H., Mean monthly values of precipitable water over the United States, 1946–56, *Mon. Weather Rev*, *88*, 25–35, 1960*a*.

Reitan, C. H., Distribution of precipitable water vapor over the continental United States, *Bull. Am. Meteorol. Soc.*, *41*, 79–87, 1960*b*.

Rind, D., E.-W. Chiou, W. Chu, J. Larsen, S. Oltmans, J. Lerner, M. P. McCormick, and L. McMaster, Positive water vapour feedback in climate models confirmed by satellite data, *Nature*, *349*, 500–503, 1991.

Telegadas, K., and J. London, A physical model of northern hemisphere troposphere for winter and summer, *Sci. Rep. 1*, contract AF19(122)-165, 55 pp., Res. Div., College of Eng., N. Y. Univ., 1954.

Tuller, S. E., World distribution of mean monthly and annual precipitable water, *Mon. Weather Rev.*, *96*, 785–797, 1968.

van de Berg, L., A. Pyomjamsri, and J. Schmetz, Monthly mean upper tropospheric humidities in cloud-free areas from Meteosat observations, *Int. J. Climatol.*, *11*, 819–826, 1991.

W. P. Elliott and D. J. Gaffen, Air Resources Laboratory, National Oceanic and Atmospheric Administration, 1325 East West Highway, Silver Spring, MD 20910.

A. Robock, Department of Meteorology, University of Maryland, College Park, MD 20742.

(Received May 12, 1992;
revised August 18, 1992;
accepted August 19, 1992.)